

Dynamical phase diagram of Gaussian BEC wave packets in optical lattices

T. Neff¹, H. Hennig², R. Fleischmann¹

¹Max Planck Institute for Dynamics and Self-Organization, 37073 Göttingen, Germany and

²Department of Physics, Harvard University, Cambridge, MA 02138, USA

(Dated: May 15, 2022)

We study the mean field dynamics of self-trapping in Bose-Einstein condensates loaded in deep optical lattices with Gaussian initial conditions. We calculate a detailed dynamical phase diagram accurately describing the different dynamical regimes (such as diffusion and self-trapping) that markedly differs from earlier predictions based on variational dynamics. The phase diagram exhibits a very complex structure which could readily be tested in current experiments. We derive an explicit theoretical estimate for the transition to self-trapping in excellent agreement with our numerical findings.

PACS numbers: 03.75.Gg, 03.75.Lm, 67.85.Hj

Introduction.—Bose-Einstein condensates (BECs) trapped in periodic optical potentials have proven to be an invaluable tool to study fundamental and applied aspects of quantum optics, quantum computing and solid state physics [1–5]. In the limit of large atom numbers per well, the dynamics can be well described by a mean-field approximation which leads to a lattice version of the Gross-Pitaevskii equation, the discrete nonlinear Schrödinger equation (DNLS) [5, 6]. One of the most intriguing features of the dynamics of nonlinear lattices is that excitations can spontaneously stably localize even for repulsive nonlinearities. This phenomenon of discrete self-trapping (ST), also referred to as the formation of *discrete breathers (DB)* or *intrinsic localized modes*, is a milestone discovery in nonlinear science that has sparked many studies (for reviews see [7, 8]). DBs have experimentally been observed in various physical systems such as arrays of nonlinear waveguides [9, 10] and Josephson junctions [11, 12], spins in antiferromagnetic solids [13, 14], and BECs in optical lattices [15]. Theoretical studies of ST of BECs in optical lattices have mainly been carried out within the mean-field approximation (that will be used in this article as well), however, ST has also been shown to exist in the dynamics of the Bose-Hubbard Hamiltonian (BHH) [16] and even in calculations beyond the BHH, which include higher-lying states in the individual wells [17, 18].

An important aspect of ST, that is far from being fully understood, is how long term stable, self trapped states get populated by general excitations. One mechanism is *self-localization (SL)* where homogeneously extended or thermalized initial conditions can excite self trapped states in the presence of boundary (or more general localized) dissipation [19, 20]. SL leads to a complex ST scenario [21] and persists beyond the mean field approximation [20, 22, 23]. Another approach is to study how generic wave packets can excite ST. In a seminal work Trombettoni and Semerzi [24, 25] developed a variational approach to study the mean field dynamics of Gaussian wave packets of BECs in optical lattices. They derived a dynamical phase diagram that separates ST from the

diffusive and a solitonic regime and which has become a standard reference not only in the field. However, a recent study [26] indicated that numerical simulations can show strong deviations from the variational dynamics and thus the phase diagram of ref. [24], therefore a theory of the ST of Gaussian wave packets is still illusive even in the mean field limit.

In this letter we identify suitable dynamical quantities that allow us to numerically differentiate the individual dynamical regimes and present a detailed dynamical phase diagram for initially Gaussian wave packets of BECs in deep optical lattices in the mean field limit. Furthermore, using the concept of the *Peierls-Nabarro energy barrier* we derive an explicit analytical expression estimating the border line between the diffusive and ST regimes that shows excellent agreement with the numerical phase diagram.

Model.—In the limit of large atom numbers per well, the dynamics of dilute Bose-Einstein condensates trapped in deep optical potentials are well described by the mean field Bose-Hubbard Hamiltonian [6, 25, 27]

$$H = \sum_{n=1}^M U |\psi_n|^4 + \mu_n |\psi_n|^2 - \frac{T}{2} \sum_{n=1}^{M-1} \psi_n^* \psi_{n+1} + c.c., \quad (1)$$

where M is the lattice size, $|\psi_n(t)|^2$ is the norm (number of atoms at site n), U denotes the onsite interaction (between two atoms at a single lattice site), μ_n is the onsite chemical potential and T is the strength of the tunnel coupling between adjacent sites. The corresponding dynamical equation is the *discrete nonlinear Schrödinger equation (DNLS)*. In its dimensionless form it reads

$$i \frac{\partial \psi_n}{\partial t} = (\lambda |\psi_n|^2 + \epsilon_n) \psi_n - \frac{1}{2} [\psi_{n-1} + \psi_{n+1}] \quad (2)$$

for $n = 1 \dots M$ with $\psi_0 = \psi_{M+1} = 0$, $\lambda = 2U/T$ and $\epsilon_n = \mu_n/T$. The DNLS describes a high dimensional chaotic dynamical system. Its dynamics, however, in general is far from being ergodic and e.g. shows localization in the form of stationary DB (localized excitations pinned to the lattice) Fig.(1d) and so called *moving breathers (MB)* traversing the lattice [28].

Examples.—The different characteristic types of dynamics are exemplified in Fig. 1: An initial condition that rapidly disperses, i.e. shows diffusive behavior, can be seen in Fig. 1a. Moving solitonic solutions are strictly speaking not supported by the DNLS [29], they emit radiation and will eventually be pinned to the lattice or diffusively spread. However, as in Fig. 1b, these losses of norm can become infinitesimally small so that these solutions remain traveling for extremely long times and can therefore be regarded as actual moving breather solutions for practical use. Finally an example of a stationary DB emerging from a Gaussian initial condition is shown in Fig. 1c. Exact DB solutions were calculated analytically in [30, 31] for a system of three sites (trimer). For larger lattices the DB solutions can be numerically calculated using the anti-continuous method [32–34] or a Newton method [35]. To prepare an experimental system in such exact breather states is usually not feasible in practice. So a prediction is needed when more general localized states, that can be easily be prepared in experiment, will show *self trapping* and remain (at least with a substantial part of their norm) localized.

Variational approach.—In [24, 25] the dynamics of Gaussian wave packets initially defined by

$$\psi_{n,0} \propto \exp \left[-\frac{(n - \xi_0)^2}{\alpha_0} + ip_0(n - \xi_0) + i\frac{\delta_0}{2}(n - \xi_0)^2 \right] \quad (3)$$

was studied using a variational collective coordinate approach (a technique very successfully applied in a variety of different fields [36, 37]). It leads to approximate equations of motion for the conjugate variables (p, ξ) and ($\delta, \sqrt{\alpha}$) [24, 25]. This variational approach (VA) assumes that the excitation is well approximated by a Gaussian at *all* times. The effective (approximate) Hamiltonian is [25]

$$H = \frac{\lambda}{2\sqrt{\pi\alpha}} - \cos(p)e^{-\eta} + V(\alpha, \xi) \quad (4)$$

with $\eta = \frac{1}{2\alpha} + \frac{\alpha\delta^2}{8}$ depending on the initial values of the center ξ_0 and width parameter $\sqrt{\alpha_0}$ as well as p_0 and δ_0 their conjugate momenta. The effective potential term $V(\alpha, \xi)$ originates from the variation of the chemical potentials from site to site, e.g. in tilted optical lattices. Here we will only discuss the case of an untilted trapping potential and hence $V(\alpha, \xi) = 0$.

Ref. [24] derived a phase diagram for the VA dynamics, predicting for which initial parameters the Gaussian wave packets would either decay, lead to solitonic moving excitations or remain localized in a self trapped state. These theoretical predictions however disagree with numerical simulations of the actual DNLS dynamics, because the final dynamical state will in most cases be highly non-Gaussian and the VA breaks down, as already pointed out recently in [26]. The examples presented above are representative cases where the VA fails. Figure 1a shows diffusion, while the VA predicts a self-trapped state for this initial condition. In Fig. 1b we find a moving breather

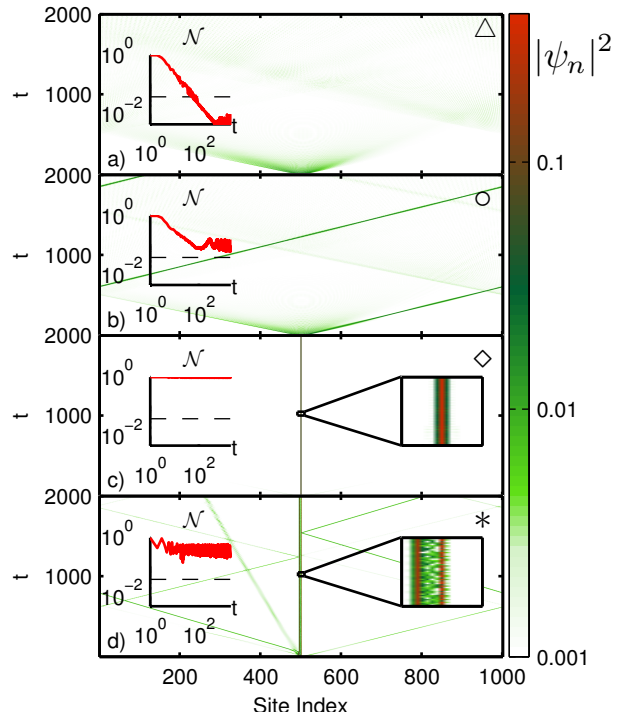


Figure 1: Examples of the different dynamical regimes. The density plots show the evolution of the norms $|\psi_n|^2$ of initially Gaussian wave packets (Eq.(3)). The insets on the left show the time traces of the maximum local norm \mathcal{N} (see Eq. 5). (a) ($\alpha_0 = 1, \cos(p_0) = 0.88, \lambda = 2.5$) strongly diffusive (VA predicts ST). (b) ($\alpha_0 = 1, \cos(p_0) = 0.88, \lambda = 1.5$) MB regime (VA predicts diffusion). (c) ($\alpha_0 = 1, \cos(p_0) = -1, \lambda = 3$) DB solution. (d) ($\alpha_0 = 4, \cos(p_0) = -0.6, \lambda = 8.9$) shows a breather of higher order with asymmetric shape. It corresponds to a drop in \mathcal{H}_{thrs} . The examples are indicated by \triangle (a), \circ (b), \diamond (c) in Fig.(2) (and * (d) in Fig.(6) in the supplemental material).

while the VA predicts diffusive behavior. Thus a complete and detailed phase diagram predicting the final dynamical state of initially Gaussian wave packets is still missing.

Order parameters.—In order to compute such a phase diagram we need criteria to distinguish the different dynamical regimes. This separation is non-trivial, as part of the atom cloud can remain trapped in one region while another part diffuses in the remainder of the lattice. It appears therefore that a single order parameter does not suffice to distinguish the different dynamical regimes. We will, however, be able to separate between the regimes by defining a local norm and local average current as

$$N_{loc}(x) = \sum_{n=x-a}^{x+a} |\psi_n|^2, \quad \text{and}$$

$$j_{loc}(x) = \left| \sum_{n=x-a}^{x+a} \frac{\hbar}{2mi} [\psi^* \nabla \psi - \psi \nabla \psi^*] \right|$$

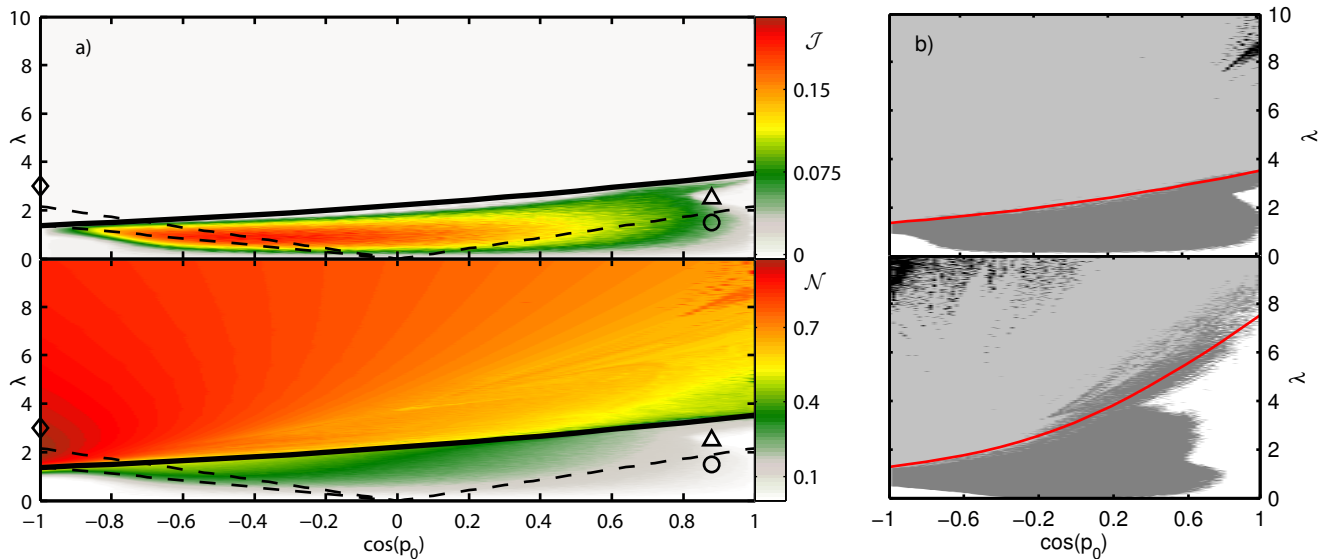


Figure 2: a) Colormap of the two order parameters \mathcal{J} (top) and \mathcal{N} (bottom) for $\sqrt{\alpha_0} = a = 1$ and system size $M = 1001$. The black dashed lines were predicted in [24] to mark the transition between different dynamical regimes. The solid line is our analytical estimate on the transition between the moving breather- and the ST regime, Eq.(7).

b) Dynamical phase diagrams of Gaussian initial conditions in the DNLS for a lattice size of $M = 1001$ and $\alpha_0 = 1$ (top) respectively $\alpha_0 = 4$ (bottom). White indicates diffusive states, light grey ST and dark grey moving breather solutions. Black indicates *higher order* more complex self-trapped solutions. The red curve represents our analytical estimate of the ST transition, Eq. 7, in excellent agreement with the numerical data.

and two order parameters by

$$\mathcal{N} = \langle \max_x (N_{loc}(x)) \rangle \quad \text{and} \quad \mathcal{J} = \langle j_{loc}(x_{max}) \rangle, \quad (5)$$

where x_{max} is the central site at which $N_{loc}(x)$ assumes its maximum. Both quantities were evaluated after an evolution time of $\tau = 10000$ and averaged over the last 10% of the time steps. The width a was chosen as the smallest integer $\geq \sqrt{\alpha_0}$. \mathcal{N} and \mathcal{J} together suffice to define the different regimes of diffusion, moving breathers and DBs. In the diffusive regime both order parameters are small. Moving breathers are characterized by large \mathcal{N} due to the localization and large \mathcal{J} because of the movement of the excitation. In the ST regime one finds large local norms but nearly vanishing currents due to the stationarity of the solutions. Fig. 2 shows \mathcal{J} and \mathcal{N} as a function of the initial phase difference p_0 and the nonlinearity λ for $\alpha_0 = 1$. (A plot for $\alpha_0 = 4$ can be found in the supplemental material.) The examples of Fig. 1 are marked in Fig. 2 by different symbols and demonstrate how the above criteria can be used to distinguish the dynamical regimes (a cut along $\cos(p_0) = 0.88$ can be found in the supplemental material). The dashed lines in Fig. 2 show the prediction of Ref. [24] of the transition between the dynamical regimes. It is clear from the figure, that the VA does not well predict the actual evolution of Gaussian initial-conditions in the DNLS. Below we will therefore use a different approach to theoretically study the ST transition of Gaussian wave packets (solid black line in Fig. 2).

Theory.—The ability of localized excitations to move

inside a lattice can be analyzed using the concept of the Peierls Nabarro energy barrier. The exact DB solution forming a single peak centered at a single lattice site (denoted *cp* for "central peak") is a local maximum in the energy. These solutions can be numerically constructed using the methods described in Refs. [32–35]. They correspond to elliptic fixed points in phase space [38] which are separated from moving and chaotic solutions by saddle points in the energy landscape. These saddle points correspond to another kind of stationary solutions centered between two lattice sites called *central bond* (cb) states. They are unstable [38] and have a lower energy content than cp-solutions. Due to continuity these solutions are assumed to be intermediate states for an excitation to hop between lattice sites. A crucial condition for a localized excitation to move across the lattice thus is that the initial energy is lower than the energy of a cb-solution such that this crossover state cannot act as a barrier. Self-trapping on the other hand requires the initial energy to be between the maximum energy state cp and cb which can now act as a barrier in phase space and inhibits migration. This energy gap between cp and cb is referred to as the Peierls Nabarro (PN) barrier [30, 38, 39]. So in other words self trapping requires a non vanishing PN barrier.

The PN barrier for excitations of norm $n = 1$ is shown in Fig. 3 Above a threshold nonlinearity of $\lambda_{PN} \approx 1.3$ the PN barrier is substantially non-zero. An important aspect to consider is that only a fraction of the norm of the initial Gaussian will actually be trapped when a

breather is created (and this norm will be smaller the further the phase differences p_0 of the Gaussian deviates from the phase difference of the breather fixed point, i.e. $p = \pi$ or $\cos(p) = -1$). The rest can either spread diffusively throughout the lattice or form smaller moving breather-like excitations. Our theoretical analysis focuses on the self trapped fraction of norm and thus the existence of a non-zero PN barrier corresponding to the respective fraction of norm n . This of course leaves the background unattended yet proves to be a valid approximation. The energy of an arbitrary state of norm n

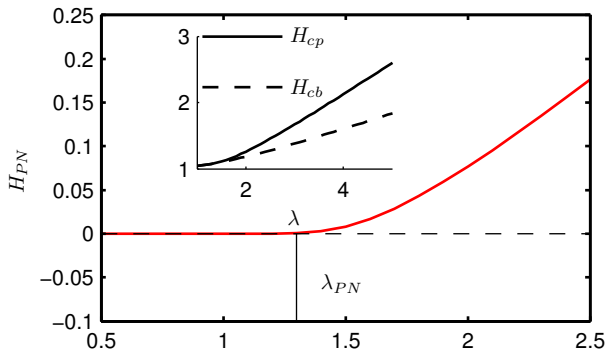


Figure 3: Peierls Nabarro energy barrier for $n = 1$ corresponding to $\lambda_{PN} = 1.3$ calculated as the difference between the energies of a bright central peak breather located around a single site (cp) and a central bond breather located between two lattice sites (cb).

compared to the state of the same shape but of unit norm scales according to $E(\lambda, n) = n \cdot E(\lambda \cdot n, 1)$, which follows directly from Eq. (1). (And it is easy to see from Eq. (2) that both states will follow the same dynamics when λ is scaled accordingly.) For the central-bond state we find $H_{cb}(\lambda, n) = n \cdot H_{cb}(\lambda \cdot n, 1) = \frac{\lambda'}{\lambda} \cdot H_{cb}(\lambda', 1)$ for $\lambda' = \lambda \cdot n$. A second condition for ST is, that the energy of the stationary solution has to be provided by our initial Gaussian, Eq. (3), because energy is a conserved quantity. It can be approximated by $H_G = \frac{\lambda}{2\sqrt{\pi\alpha_0}} - \cos(p_0)e^{-\eta_0}$ with $\eta_0 = \frac{1}{2\alpha_0}$ [24], which we found to agree very well with the numerically obtained values for the exact DNLS energy H . In accordance with our two criteria we make the following Ansatz to estimate λ_c , the critical nonlinearity at the transition to self trapping:

$$H_{cb}(\lambda_c, n_c) = \frac{\lambda_{PN}}{\lambda_c} \cdot H_{cb}(\lambda_{PN}, 1) = \frac{\varepsilon}{\lambda_c} \stackrel{!}{=} H_G(\lambda_c) \quad (6)$$

where $\varepsilon = \lambda_{PN} \cdot H_{cb}(\lambda_{PN}, 1)$. We extract ε from Fig. 3 where we find the cb-energy at λ_{PN} to be $H_{cb}(\lambda_{PN}, 1) \approx 1.0723$ leading to $\varepsilon \approx 1.37$. With this we obtain

$$\lambda_c = e^{-\eta} \sqrt{\pi\alpha_0} \cos p_0 + \sqrt{e^{-2\eta} \pi\alpha_0 \cos^2 p_0 + 2\varepsilon \sqrt{\pi\alpha_0}} \quad (7)$$

providing a theoretical estimate for the transition to the ST regime (Fig. 2). For a phase difference of $p_0 = \pi$, i.e.

matching the fixed point phase difference, these two conditions indicate the transition between the two regimes at $n_c \approx 0.95$ and $\lambda_c \approx 1.35$. If we compare this theoretical prediction with the numerical data in Fig.(2), from which we read $\lambda_c = 1.35$, we find an excellent agreement. For other phase differences the norm that self traps is smaller, however, we still find very good agreement with the numerical data.

Phase diagram.—Finally we construct the dynamical phase diagram which assigns every initial condition to a specific dynamical regime by defining suitable thresholds for our order parameters \mathcal{N} and \mathcal{J} . Figure 2 shows remarkably sharp transitions in the maximum local probability current. Therefore \mathcal{J} was used as a principal indicator required to be very low for ST. We fix $\mathcal{J}_{thrs} = 0.002$ as the border for the ST regime. \mathcal{N} on the other hand can be used to delimit the diffusive regime [40] To this purpose we calculated the probability density function (pdf) of \mathcal{N} (see supplemental material) in the diffusive case where the single site norms are known to be exponentially distributed [21] in a purely stochastic approach. We consider a specific initial condition which leads to vanishing current to be self-trapped if its evolution leads to a maximum local norm \mathcal{N} that is sufficiently unlikely to be found in any diffusive state. As the threshold \mathcal{N}_{thrs} we define the norm where the pdf of \mathcal{N} falls below $p_T = 10^{-4}$ [41]. We find $\mathcal{N}_{thrs} = 0.028$ for $\alpha_0 = 1$ and $\mathcal{N}_{thrs} = 0.032$ for $\alpha_0 = 4$. With this thresholds we obtain the dynamical phase diagram shown in Fig. 2b. It is strikingly different from the prediction of the VA, however, the observed ST transition is in excellent agreement with Eq. (7) (solid black line).

To identify higher order self-trapped excitations of more complex structure (see Fig. 1d) in our phase diagram, we use a third order parameter, the local energy $H_{loc}(x) = \sum_{n=x-a}^{x+a} \frac{\lambda}{2} |\psi_n|^4 - \sum_{n=x-a-1}^{x+a} \frac{1}{2} (\psi_n^* \psi_{n+1} + c.c.)$ in the vicinity of x_{max} measured against the fixed point energy, i.e. $\mathcal{H}(\lambda) = H_{loc}(x_{max})/H_{cp}(\lambda, 1)$. For higher order the ST we found $\mathcal{H} \ll 1$ in contrast to $\mathcal{H} \approx 1$ for DB centered around a single site. We chose $\mathcal{H}_{thrs} = 0.8$ and marked this regime in black in Fig. 2b.

In conclusion we have studied the dynamics of Bose Einstein Condensates in periodic optical potentials calculating a detailed phase diagram for the dynamics of Gaussian initial conditions. It not only separates the different dynamical regimes (diffusive, moving breathers, self-trapping) but also shows the emergence of higher order self-trapped breather states. We derived an explicit expression for the nonlinearity strength at the transition to the ST regime, in very good agreement with the numerical data. Gaussian initial conditions can be well controlled in experiments on BECs [5] and our predictions can therefore readily be tested experimentally. Our results do not only apply to BECs, however, but to all the various systems described by the DNLS. For BECs it poses an interesting open question how correlations will affect the phase diagram beyond the mean-field descrip-

tion of the DNLS.

We thank Jérôme Dornigac for useful discussions.

Acknowledgments

HH acknowledges financial support by the German Research Foundation (DFG), grant no. HE 6312/1-1.

-
- [1] I. Bloch, *Nat. Phys.* **1**, 23 (2005).
- [2] W. S. Bakr, J. I. Gillen, A. Peng, S. Fölling, and M. Greiner, *Nature* **461**, 74 (2009).
- [3] W. S. Bakr, A. Peng, M. E. Tai, R. Ma, J. Simon, J. I. Gillen, S. Fölling, L. Pollet, and M. Greiner, *Science* **329**, 547 (2010).
- [4] J. Simon, W. S. Bakr, R. Ma, M. E. Tai, P. M. Preiss, and M. Greiner, *Nature* **472**, 307 (2011).
- [5] O. Morsch and M. Oberthaler, *Rev. Mod. Phys.* **78**, 179 (2006).
- [6] C. J. Pethick and H. Smith, *Bose-Einstein Condensation in Dilute Gases* (Cambridge University Press, 2008).
- [7] S. Flach and C. R. Willis (1997).
- [8] D. Campbell, S. Flach, and Kishar, Yuri, *Physics Today* (2004).
- [9] H. S. Eisenberg, Y. Silberberg, R. Morandotti, A. R. Boyd, and J. S. Aitchison, *Phys. Rev. Lett.* **81**, 3383 (1998).
- [10] R. Morandotti, U. Peschel, J. S. Aitchison, H. S. Eisenberg, and Y. Silberberg, *Phys. Rev. Lett.* **83**, 2726 (1999).
- [11] E. Trias, J. J. Mazo, and T. P. Orlando, *Phys. Rev. Lett.* **84**, 741 (2000).
- [12] A. V. Ustinov, *Chaos* **13**, 716 (2003).
- [13] U. T. Schwarz, L. Q. English, and A. J. Sievers, *Phys. Rev. Lett.* **83**, 223 (1999).
- [14] M. Sato and A. J. Sievers, *Nature* **432**, 486 (2004).
- [15] B. Eiermann, T. Anker, M. Albiez, M. Taglieber, P. Treutlein, K.-P. Marzlin, and M. K. Oberthaler, *Phys. Rev. Lett.* **92**, 230401 (2004).
- [16] H. Hennig, D. Witthaut, and D. K. Campbell, *Physical Review A* **86**, 051604 (2012).
- [17] K. Sakmann, A. I. Streltsov, O. Alon, and L. S. Cederbaum, *Phys. Rev. Lett.* **103**, 220601 (2009).
- [18] M. Trujillo-Martinez, A. Posazhennikova, and J. Kroha, *Phys. Rev. Lett.* **103**, 105302 (2009).
- [19] R. Livi, R. Franzosi, and G.-L. Oppo, *Physical Review Letters* **97** (2006), ISSN 0031-9007.
- [20] H. Hennig and R. Fleischmann, *Physical Review A* **87**, 033605 (2013).
- [21] G. S. Ng, H. Hennig, R. Fleischmann, T. Kottos, and T. Geisel, *New Journal of Physics* **11**, 073045 (2009), URL <http://stacks.iop.org/1367-2630/11/i=7/a=073045>.
- [22] D. Witthaut, F. Trimborn, H. Hennig, G. Kordas, T. Geisel, and S. Wimberger, *Phys. Rev. A* **83**, 063608 (2011).
- [23] F. Trimborn, D. Witthaut, H. Hennig, G. Kordas, T. Geisel, and S. Wimberger, *The European Physical Journal D* **63**, 63 (2011), ISSN 1434-6060, 1434-6079, URL <http://link.springer.com/article/10.1140/epjd/e2011-10702-7>.
- [24] A. Trombettoni and A. Smerzi, *Phys. Rev. Lett.* **86**, 2353 (2001).
- [25] A. Smerzi and A. Trombettoni, *Journal Of Physics B* **34**, 4711 (2001).
- [26] R. Franzosi, R. Livi, G.-L. Oppo, and A. Politi, *Nonlinearity* **24**, R89 (2011), URL <http://stacks.iop.org/0951-7715/24/i=12/a=R01>.
- [27] P. Buonsante and V. Penna, *Journal of Physics A: Mathematical and Theoretical* **41**, 175301 (2008), URL <http://stacks.iop.org/1751-8121/41/i=17/a=175301>.
- [28] S. Flach and K. Kladko, *Physica D: Nonlinear Phenomena* **127**, 61 (1999).
- [29] O. F. Oxtoby and I. V. Barashenkov, *Phys. Rev. E* **76**, 036603 (2007).
- [30] H. Hennig, J. Dornigac, and D. K. Campbell, *Phys. Rev. A* **82**, 053604 (2010).
- [31] S. Darmanyan, A. Kobayakov, and F. Lederer, *Journal of Experimental and Theoretical Physics* **86**, 682 (1998), ISSN 1063-7761.
- [32] S. Flach and A. V. Gorbach, *Physics Reports* **467**, 1 (2008), ISSN 0370-1573, URL <http://www.sciencedirect.com/science/article/pii/S0370157308001580>.
- [33] S. Aubry, *Physica D: Nonlinear Phenomena* **103**, 201 (1997), ISSN 0167-2789, URL <http://www.sciencedirect.com/science/article/pii/S0167278996002618>.
- [34] J. L. Marin and S. Aubry, *Nonlinearity* **9**, 1501 (1996), URL <http://stacks.iop.org/0951-7715/9/i=6/a=007>.
- [35] LaurentProvile and S. Aubry, *European Physical Journal BCondensed Matter and* (2000), URL <http://arxiv.org/abs/cond-mat/0004416>.
- [36] D. K. Campbell, J. F. Schonfeld, and C. A. Wingate, *Physica D: Nonlinear Phenomena* **9**, 1 (1983), ISSN 0167-2789, URL <http://www.sciencedirect.com/science/article/pii/0167278983902890>.
- [37] D. K. Campbell, *Annals of Physics* **129**, 249 (1980), ISSN 0003-4916, URL <http://www.sciencedirect.com/science/article/pii/0003491680903887>.
- [38] B. Rumpf, *Phys. Rev. E* **70**, 016609 (2004).
- [39] Y. S. Kivshar and D. K. Campbell, *Phys. Rev. E* **48**, 3077 (1993).
- [40] Note that \mathcal{J} cannot be used here, as it is small for both self-trapped and diffusive states.
- [41] Again our results are not sensitive to the exact value of this parameter p_t , in the supplement we supply a phase diagram obtained with 10^{-5} for comparison.

I. SUPPLEMENTAL MATERIAL

A cut through the phase diagram.—The phase diagram of Fig. 2 shows a remarkable transition from diffusive to moving breather behavior back to diffusive motion and than to self trapping for $\cos(p_0) \cong 0.88$. In Fig. 4 we shows curves of the order parameters as a function of the nonlinearity λ for $\cos(p_0) = 0.88$, illustrating the sharp features in the order parameters at the transitions between the different regimes.

Defining \mathcal{N}_{thrs} —In order to find a suitable upper threshold of the maximal local norm in the diffusive regime we calculate the cumulative probability density function (pdf) of \mathcal{N} in the diffusive case where the single site norms are known to be exponentially distributed $p = M \cdot e^{-Mx}$ [21]. Assuming statistical independents in this regime gives the pdf of the maximum single site norm as $p_{max} = M^2(1 - \exp(-Mx))^{M-1} \cdot \exp(-Mx)$. A DB however is localized over several sites around the maximum. Therefore we need to calculate the PDF of the local norm within a range of a sites on either side of the maximum. The PDF of the sum of two single-site norms is given by the convolution of the two PDFs. For r sites with exponentially distributed norms we can thus calculate the PDF of norms iteratively by $p_r = p_{r-1} * p$, where $*$ denotes convolution. The PDF of the local norm in the range of $2a$ sites around the maximum can consequently be expressed as $p_{\mathcal{N}} = p_{2a} * p_{max}$. Let us examine an initial condition which leads to vanishing current \mathcal{J} . We will consider it to be self-trapped if its evolution leads to a maximum local norm \mathcal{N} that is sufficiently unlikely to be found in the diffusive state. We define as the threshold \mathcal{N}_{thrs} the norm for which the PDF falls below $p_T = 10^{-4}$. We find $\mathcal{N}_{thrs} = 0.028$ for $\alpha_0 = 1$ and $\mathcal{N}_{thrs} = 0.032$ for $\alpha_0 = 4$. However, our results are not sensitive to the exact value of this parameter p_T . As-

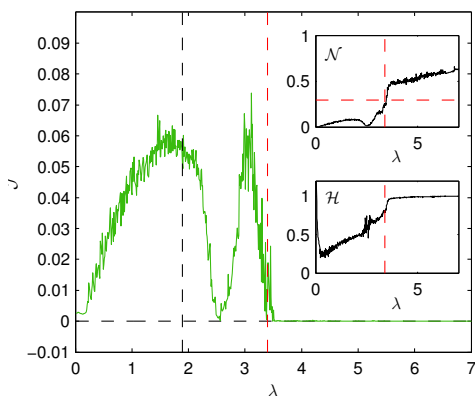


Figure 4: Crosssection through Fig.(2) at $\cos(p_0) = 0.88$. The black vertically dashed line corresponds to the predicted transition between the MB- and the DB regime of [24], the red vertically dashed lines indicate our prediction Eq.(7). The horizontal red line in the \mathcal{N}_{thrs} - inset denotes the critical norm at the transition from our analytics in very good agreement with the numerical data.

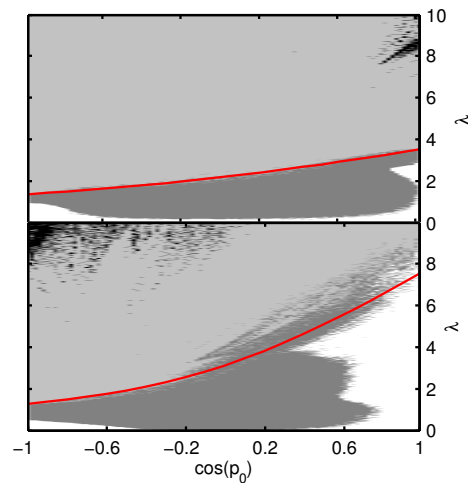


Figure 5: Phaseportraits (left) $M = 1001$ $\alpha_0 = 1$, (right) $M = 1001$ $\alpha_0 = 4$ obtained with a pdf threshold of the maximum local norm of $p_t = 10^{-5}$.

suming $p_T = 10^{-5}$ yields $\mathcal{N}_{thrs} = 0.031$ for $\alpha_0 = 1$ and $\mathcal{N}_{thrs} = 0.035$ for $\alpha_0 = 4$ which result in the phase diagrams shown in Fig. 5, which differ only minimally from those of Fig. 2b.

Order parameters for $\alpha = 4$ —Figure 6 shows the three order parameters \mathcal{J} , \mathcal{H} and \mathcal{N} for $\alpha = 4$, which give rise to the phaseportrait for $\alpha = 4$ Fig. 2b (bottom).

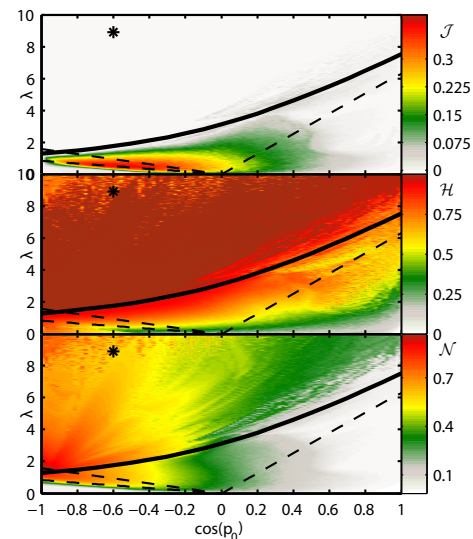


Figure 6: Colormap of the the three parameters \mathcal{J} (top), \mathcal{H} (middle) and \mathcal{N} (bottom) for $\sqrt{\alpha_0} = a = 2$ and system size $M = 1001$. The black dashed lines where predicted in [24] to mark the transition between different dynamical regimes. The solid line is our analytical estimate on the transition between the moving breather- and the ST regime, Eq.(7).